	R^2
EPL replicates	0.84
EBM3 replicates	0.83
EpiSC5 (cloneO) replicates	0.76
EpiSC7 replicates	0.91
EpiSC5 vs EpiSC7	0.92
EBM6 replicates	0.87
Gsc+Sox17–Mesoderm replicates	0.94
Gsc+Sox17+Endoderm replicates	0.94
Myoblast replicates	0.90
iPSC1D4 vs iPSC2D4	0.97
piPSC1A2 vs piPSC1B3	0.98
piPSC1B3 vs piPSCV3	0.92
piPSCV3 vs piPSC1A2	0.92
MEF (f) vs MEF (m)	0.92

Supplemental Figure 1. Correlation Coefficients between Biological Replicate Pairs or Pairs of Identical Cell Types

Shown are R^2 values between two biological replicates for a given cell line or between pairs of identical cell types, as indicated. Smoothed data for all probes were used for the calculation.

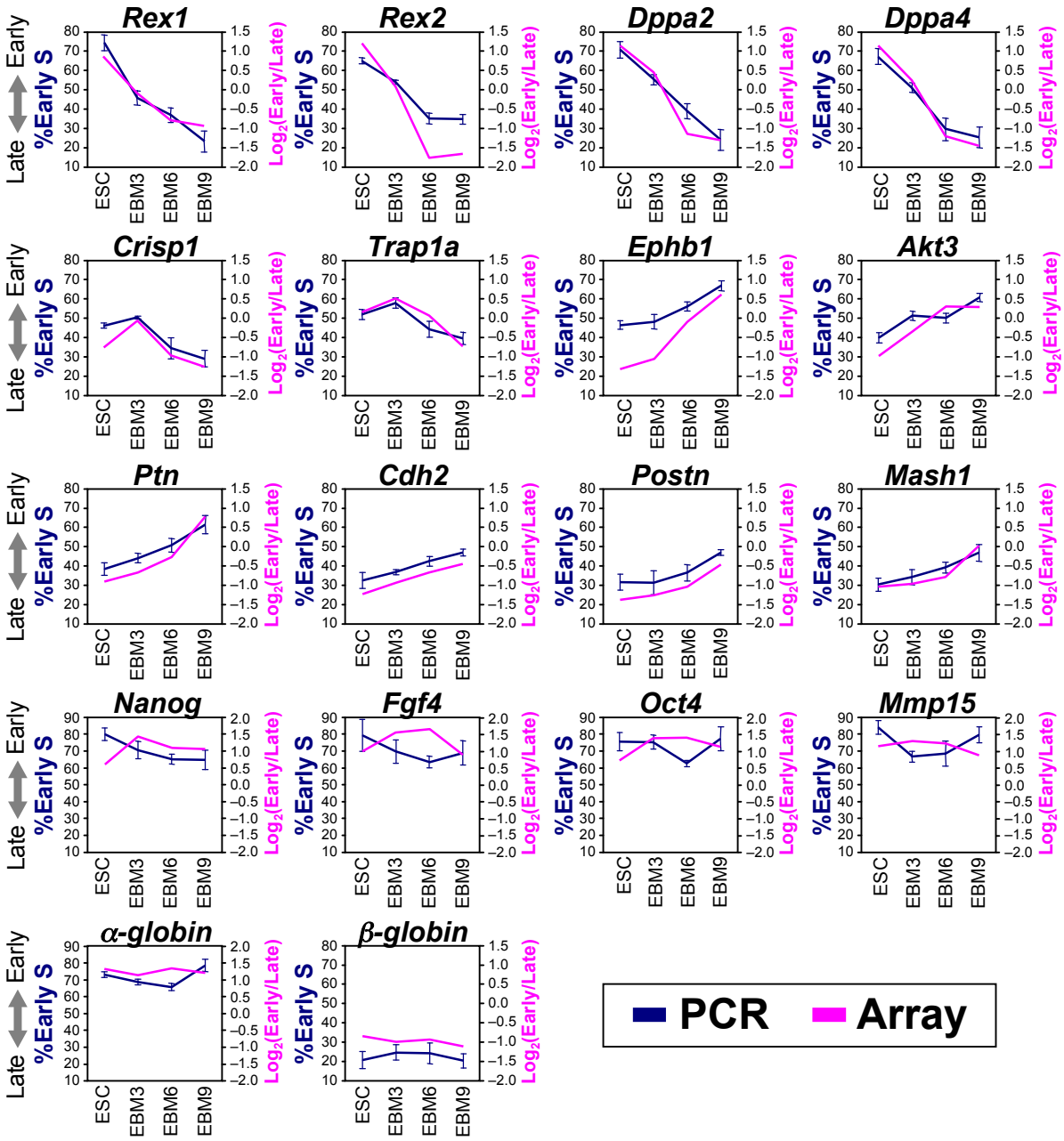

Supplemental Figure 2. Validation of Microarray-based Replication Timing Analysis by PCR
Replication timing analysis of 18 genes by individual gene PCR. Pairs of immunoprecipitated BrdU DNA samples from early and late S fractions were subject to PCR and mean % early S-phase values [=(intensity of early fraction)/(intensity of early and late fractions combined)] from 6–7 pairs of DNA samples were calculated (left y-axis; dark blue lines), as described (Hiratani et al. 2004). Error bars represent standard error of the mean. From microarray data, replication-timing ratios of genes were calculated from the loess-smoothed curve at the transcription start sites (right y-axis; magenta lines).

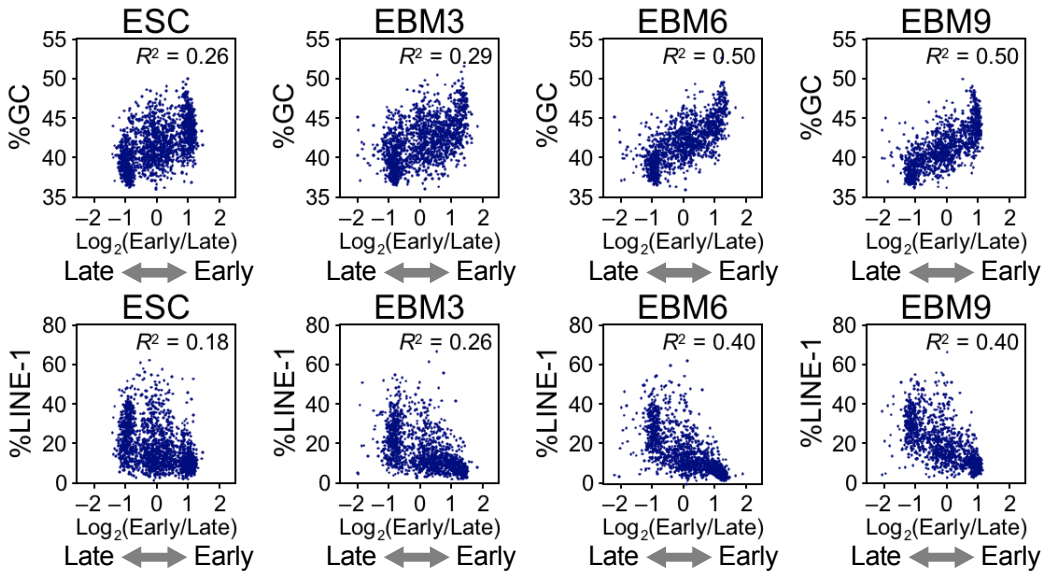

Supplemental Figure 3. Scatter Plots of Average Replication Timing Ratios of Replication Domains Versus Their GC and LINE-1 Content in ESC, EBM3, EBM6 and EBM9

Plots correspond to data shown in Figure 2E and graphically illustrate the sharp increase in Pearson's R^2 values primarily during the EBM3–EBM6 transition that indicates a genome-wide alignment of replication timing to isochore DNA sequence features, GC and LINE-1 Content.

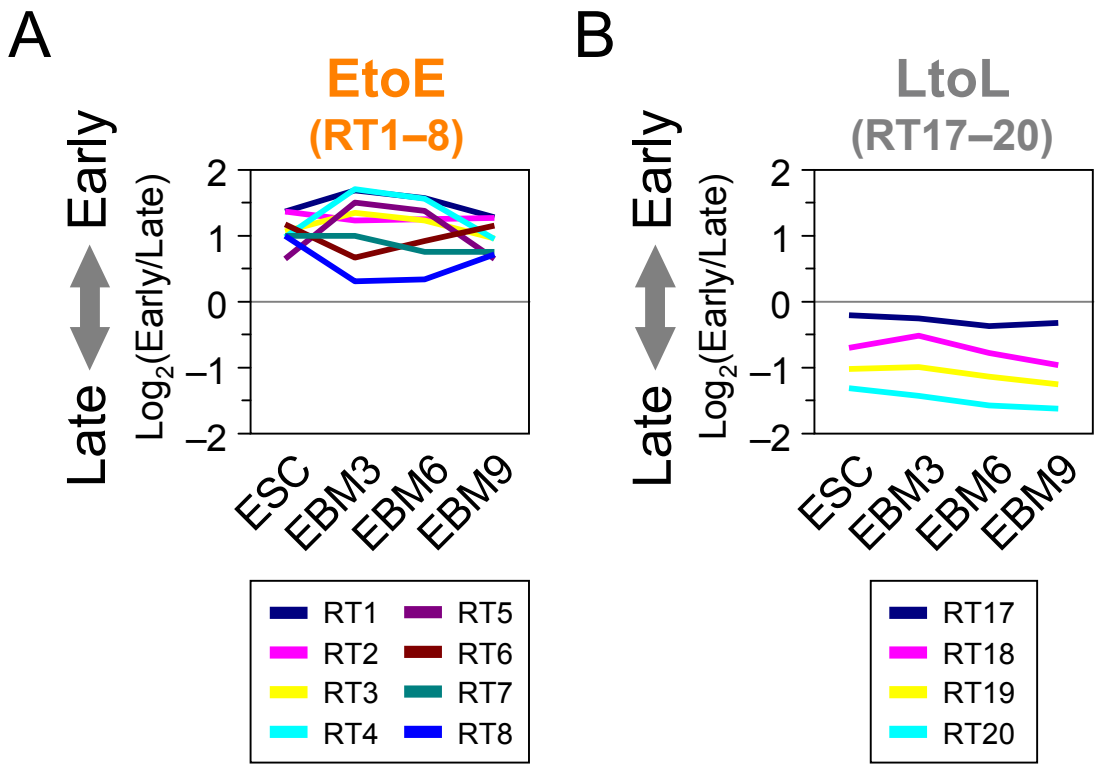

Supplemental Figure 4. Kinetics of EtoE and LtoL Replication Timing Clusters
Clusters not shown in Figure 2 are illustrated. (A) Kinetics of EtoE (RT1–8) clusters. (B) Kinetics of LtoL (RT17–20) Clusters. See Figures 2G and 2H for kinetics of LtoE (RT9–12) and EtoL (RT13–16) clusters, respectively.

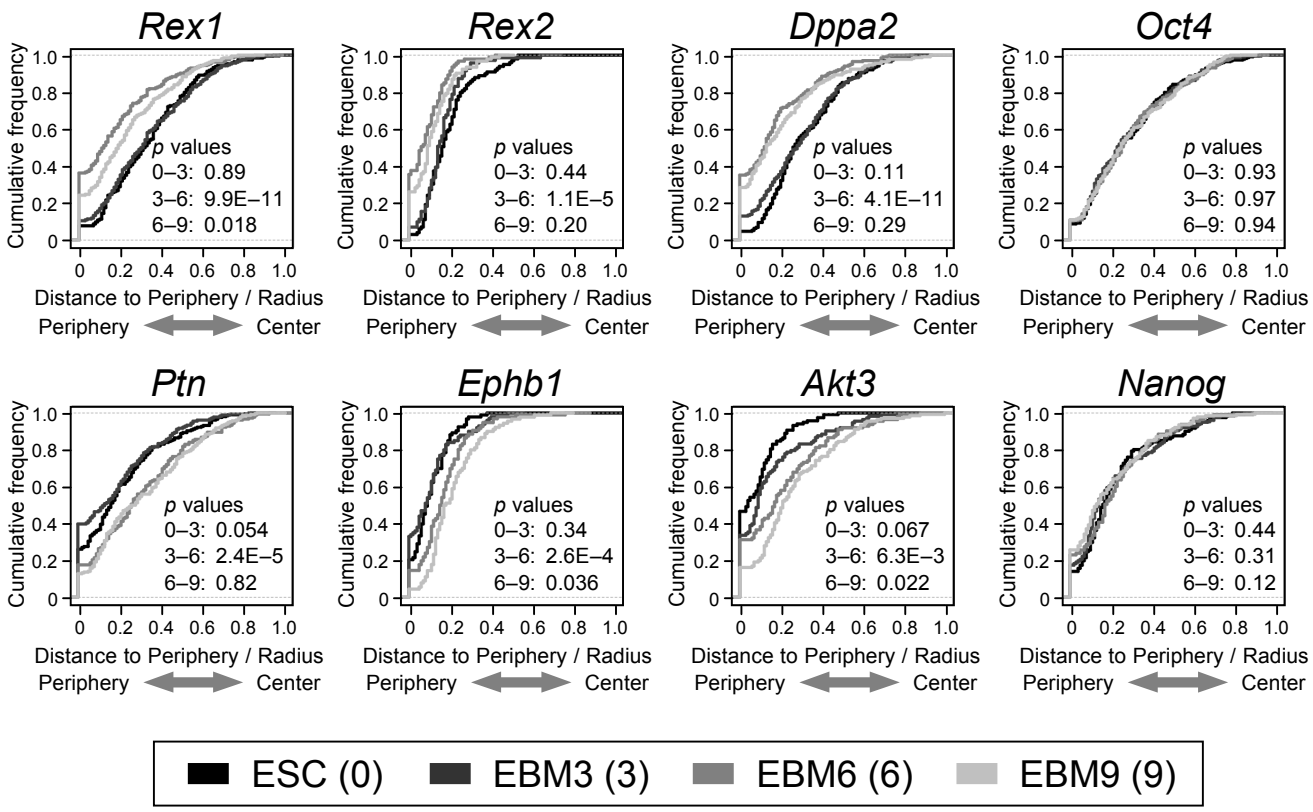

Supplemental Figure 5. Chromosomal Segments That Change Replication Timing Are Repositioned in the Nucleus During the EBM3–EBM6 Transition

3D DNA-FISH results from Figure 3 presented in the form of cumulative frequency plots. X-axis shows relative radial distance to the nuclear periphery, where 0 and 1 represents the periphery and the center of the nucleus, respectively. Note that late-replicating sequences generally show a noticeably higher number of FISH signals precisely at the periphery in 3D DNA-FISH, which have a relative radial distance of zero. This is consistent with results reported for the late-replicating *Mash1* locus in ESCs (Williams et al. 2006). *P*-values were obtained from a two-sample Kolmogorov-Smirnov test.

A

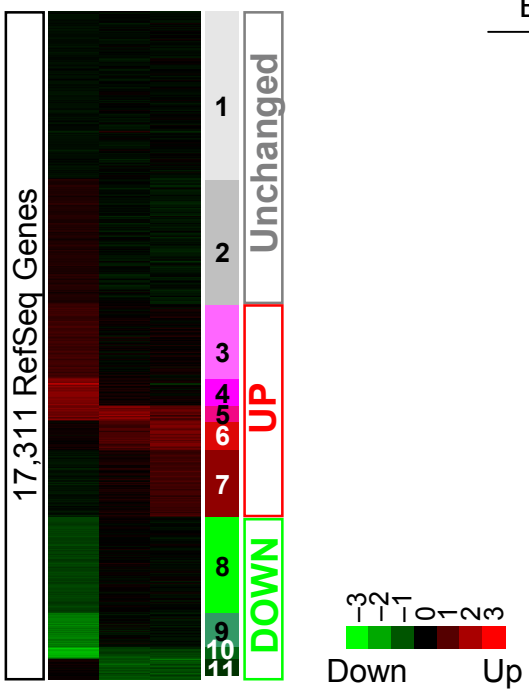

B

R^2	EBM3	EBM6	EBM9
D3ESC	0.91	0.87	0.81
EBM3		0.94	0.86
EBM6			0.91

Supplemental Figure 6. The EBM3–EBM6 Transition Is Accompanied by The Least Degree of Gene Expression Changes

(A) A heatmap showing Log_2 transformed fold changes in expression levels of 17,311 RefSeq genes in 3-day intervals. The heatmap format is identical to Figure 1C, except that Log_2 transformed values for the ratio of EBM3/ESC, EBM6/EBM3, and EBM9/EBM6 are shown. Note the least amount of green and red during the EBM3–EBM6 transition, indicating the least number of transcriptional changes during this period. (B) Pearson's R^2 values for pair-wise comparisons of expression data for 17,311 RefSeq genes. This analysis confirmed statistically that the EBM3–EBM6 transition experienced the least degree of transcriptional changes.

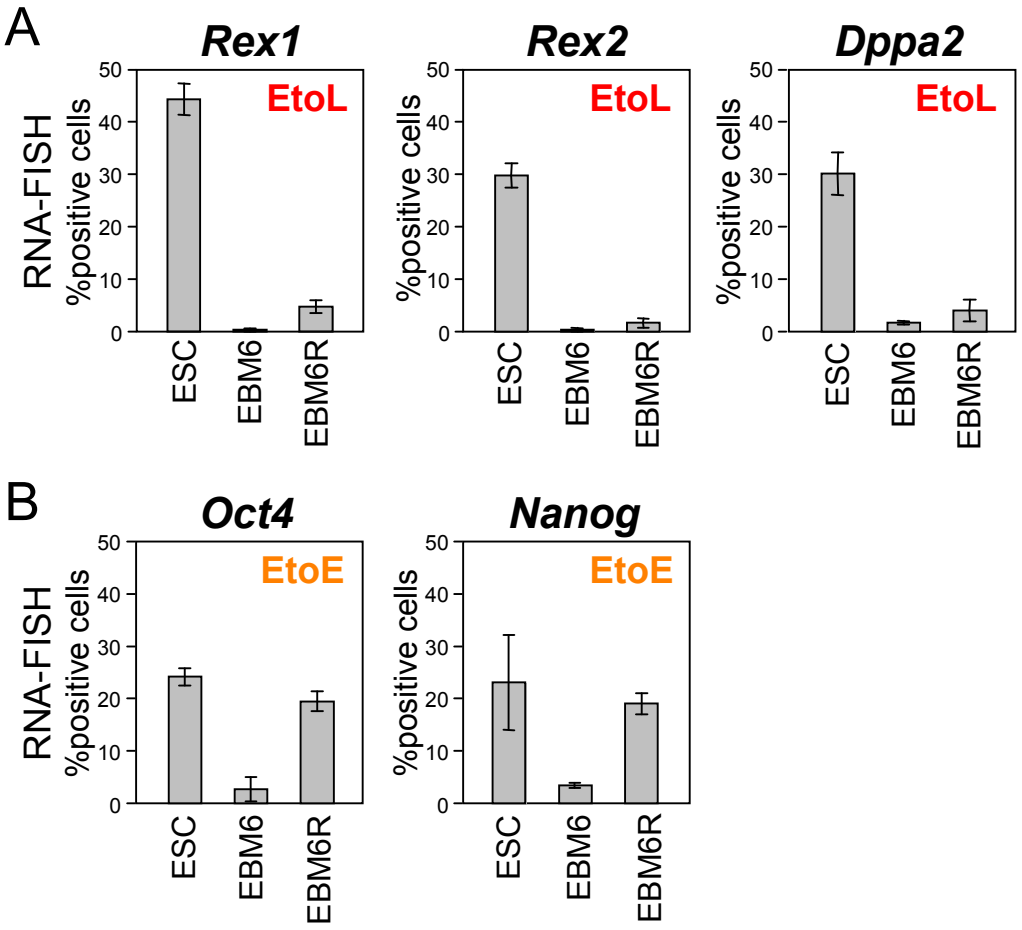

Supplemental Figure 7. Down-regulated Genes that Had Changed Replication Time and Subnuclear Position Are Difficult to Up-regulate

(A,B) Analysis of nascent transcription in ESC, EBM6 and EBM6R (defined in Fig. 4E) by RNA-FISH. Bars show % positive cells. Comparable results were obtained from three biological replicates and the sum of all experiments is shown. At least 200 cells were counted per state. Error bars represent standard error of the mean. This analysis shows that upon EtoL changes, *Rex1*, *Rex2* and *Dppa2*, become difficult to up-regulate in EBM6R (A), whereas EtoE genes, *Oct4* and *Nanog*, are up-regulated (B).

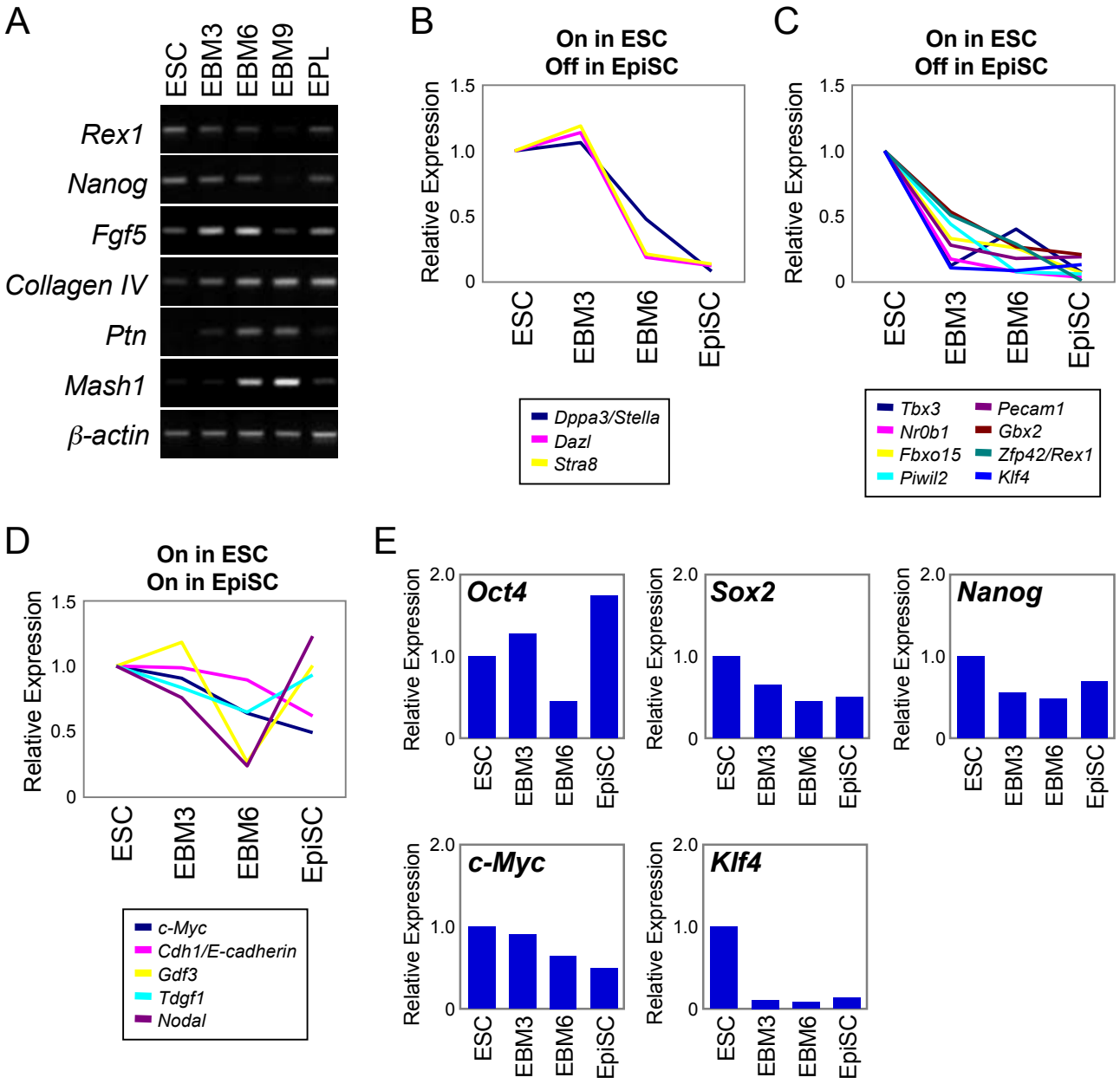

Supplemental Figure 8. Pluripotency Gene Expression Profiles in EPL cells, EBM3 and EpiSCs
(A) Similar expression profiles of EPL cells and EBM3 as assayed by RT-PCR of developmentally regulated genes. *Beta-actin*, loading control. (B,C) Relative expression levels of genes that are on in ESCs and off in EpiSCs as assayed by gene expression microarrays for ESC, EBM3, EBM6 and EpiSCs. ESC levels were defined as the baseline. While several such genes are still expressed in EBM3 (B), many are down-regulated already in EBM3 (C). (D) Relative expression levels of genes that are expressed in both ESCs and EpiSCs. These genes are expressed in EBM3. List of genes in B–D are from Figure 3A of Tesar et al (Tesar et al. 2007). (E) Pluripotency circuitry transcription factors, *Oct4*, *Sox2* and *Nanog*, are expressed in EpiSCs as well as EBM3, as assayed by microarrays. One of the reprogramming factors, *c-Myc*, is present in both EBM3 and EpiSCs, while another one, *Klf4*, is down-regulated in both. ESC levels were defined as the baseline.

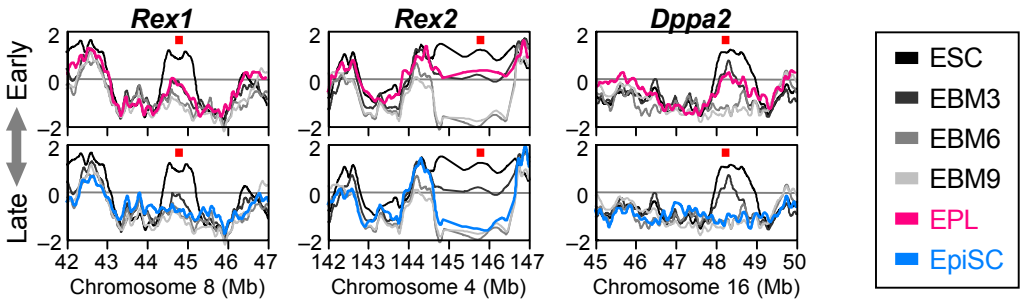

Supplemental Figure 9. Replication Profiles of EPL Cells and EpiSCs Resemble EBM3 and EBM6, Respectively

Replication timing profiles of EPL cells (magenta) or EpiSCs (blue) are overlaid on those of ESC, EBM3, EBM6 and EBM9. Three EtoL domains are shown. Representative gene name within the domains are shown with their positions in red squares.

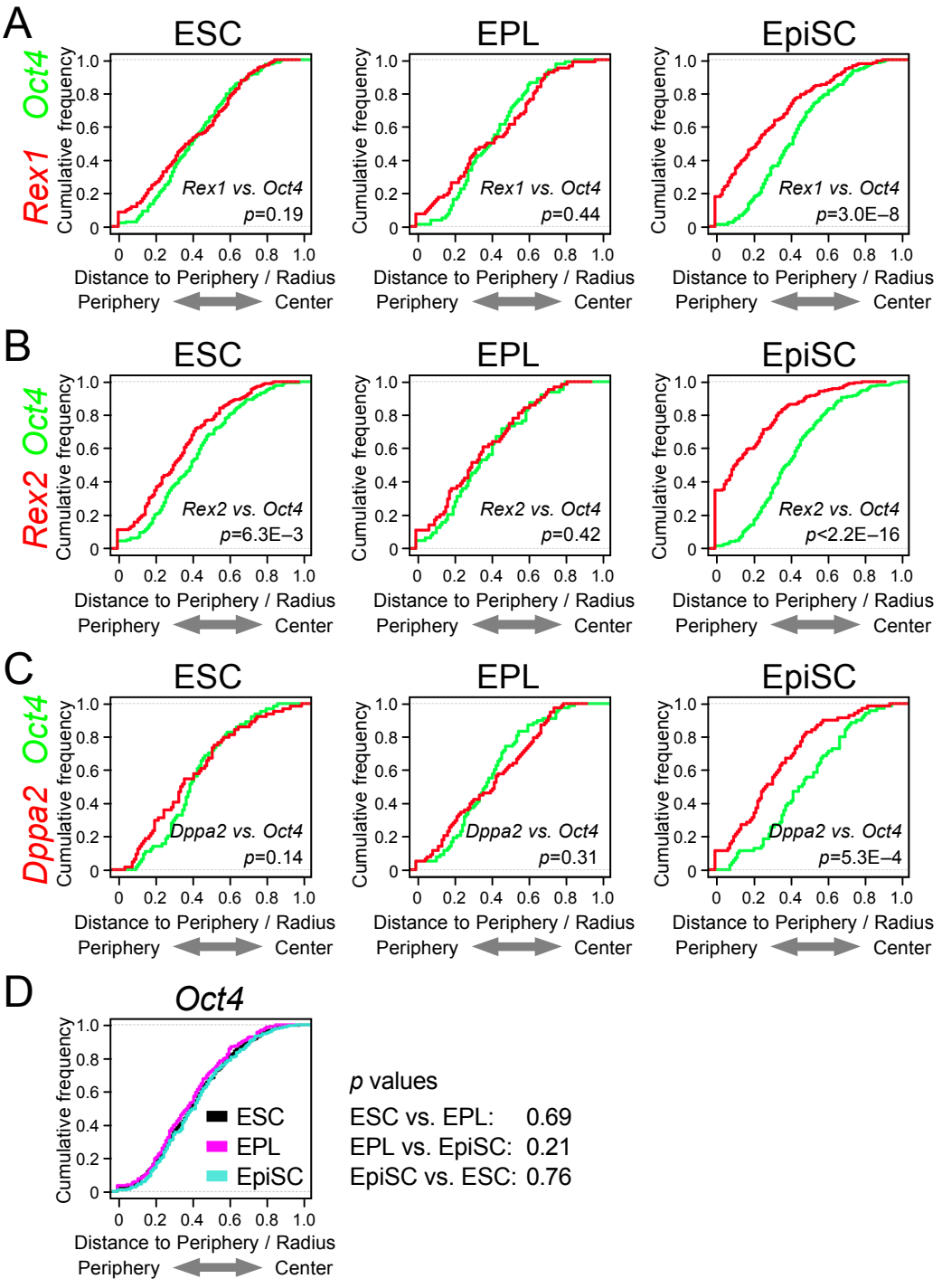

Supplemental Figure 10. Cumulative Frequency Plots of 2D DNA-FISH Analyses of ESCs, EPL cells and EpiSCs

(A–D) Two-color 2D DNA-FISH results from Figures 5D–I presented in the form of cumulative frequency plots. X-axis shows relative radial distance to the nuclear periphery, where 0 and 1 represents the periphery and the center of the nucleus, respectively. *Rex1* (A), *Rex2* (B) and *Dppa2* (C), shown in red, are significantly repositioned toward the nuclear periphery relative to *Oct4* (green) in EpiSCs compared to ESCs or EPL cells. Meanwhile, *Oct4* maintains its internal positioning in ESCs, EPL cells and EpiSCs (D). *P*-values were obtained from a two-sample Kolmogorov-Smirnov test.

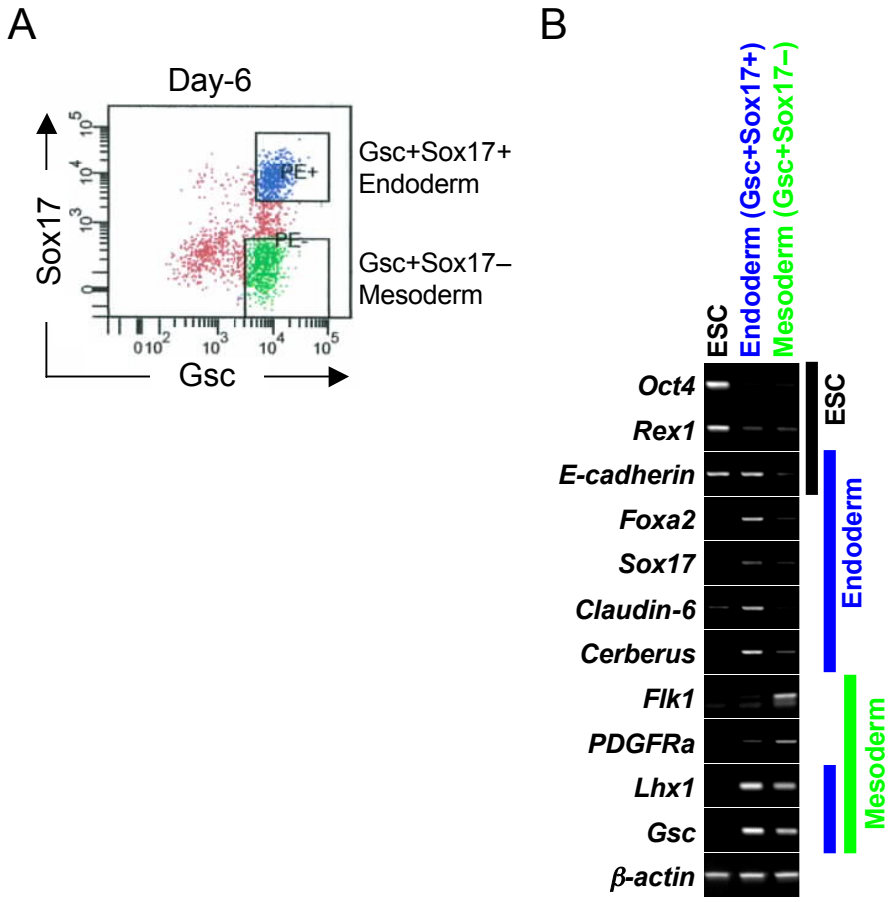

Supplemental Figure 11. Isolation and Characterization of ESC-derived Mesoderm and Endoderm Cells

(A) A FACS profile of cells after 6 days of ESC differentiation. Gsc+Sox17– mesoderm and Gsc+Sox17+ endoderm cells were isolated by flow cytometry. (B) Expression profiles of Gsc+Sox17– mesoderm progenitors and Gsc+Sox17+ endoderm progenitors as assayed by RT-PCR of markers specific to ESCs, endoderm progenitors, mesoderm progenitors, or a combination of two. ESCs are shown alongside for comparison. Gene expression microarray data for Gsc+Sox17– mesoderm and Gsc+Sox17+ endoderm is also provided in Supplemental Table 1. *Beta-actin*, loading control.

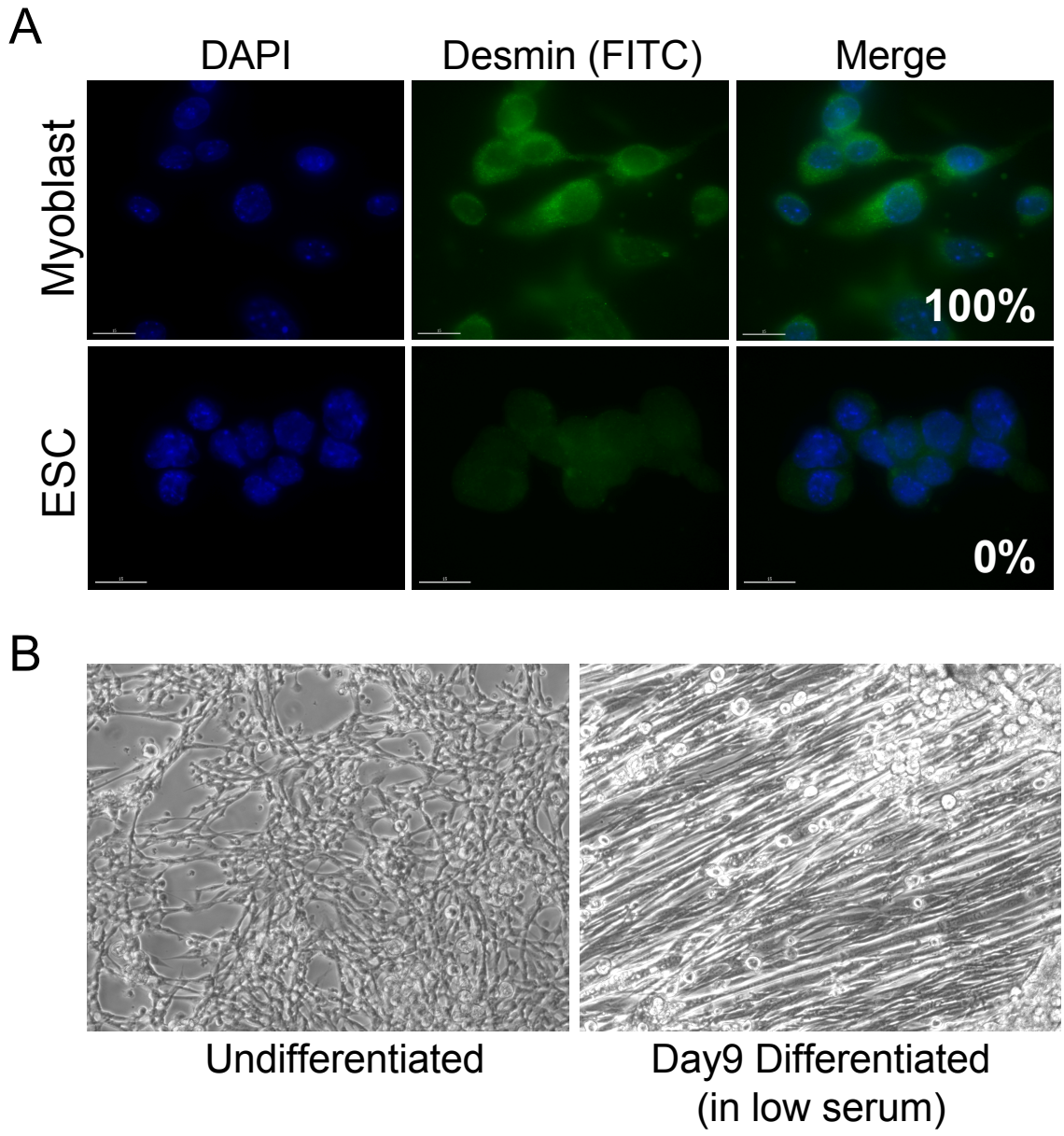

Supplemental Figure 12. Characterization of Myoblast Cells
(A) J185a myoblast cells are positive for the myoblast marker, Desmin, as assayed by immunofluorescence (Mouse anti-Desmin clone D33, Dako M0760; 1:50). ESCs serve as a negative control. (B) Culture of J185a myoblasts in low serum medium (2% horse serum) induced extensive differentiation of these cells into fused myotubes, demonstrating the myoblast identity of J185a cells.

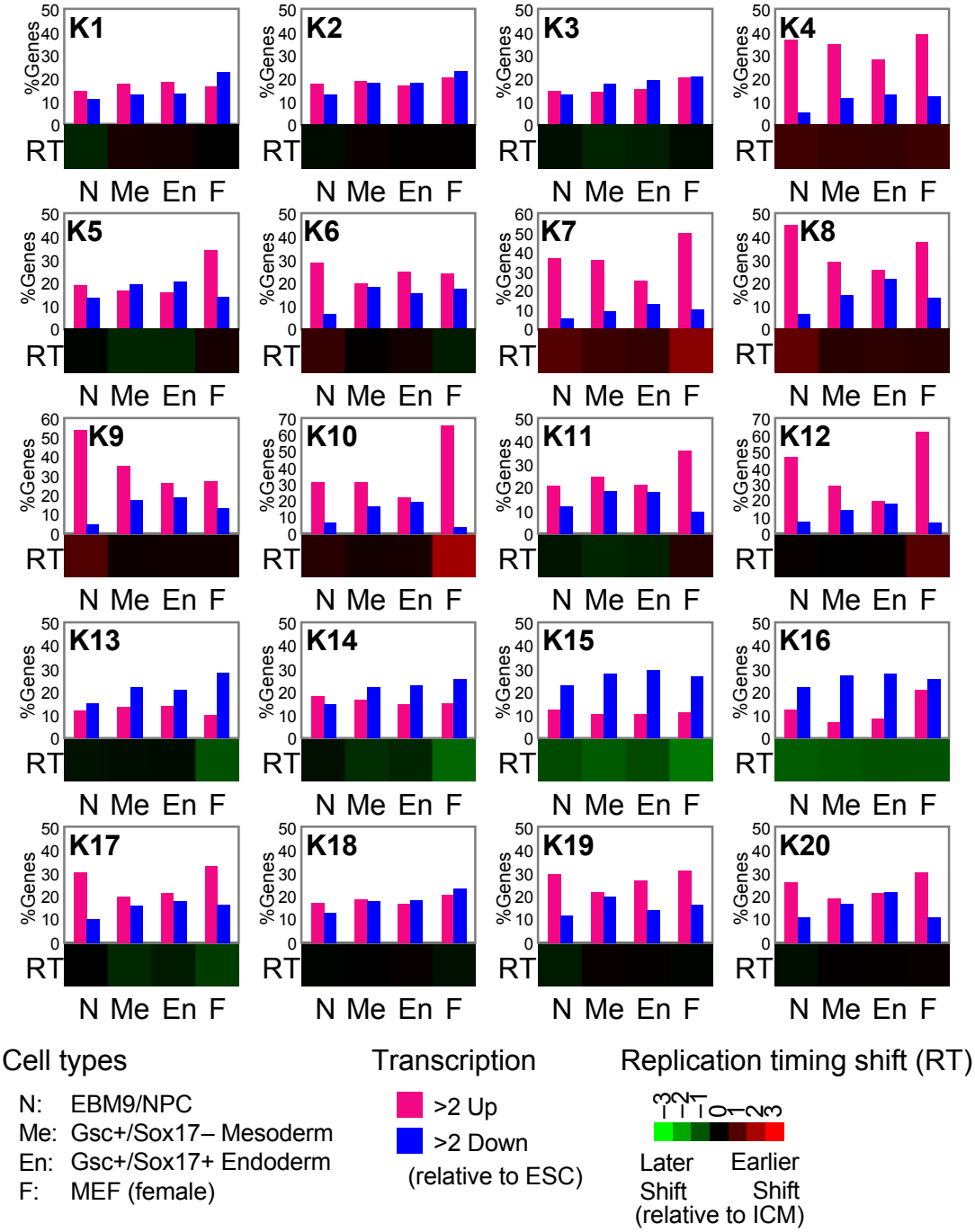

Supplemental Figure 13. LtoE and EtoL Changes Are Associated with Transcriptional Up- and Down-regulation, Respectively

Bar graphs show the percentages of 2-fold up- (red) and down-regulated (blue) genes within K-means clusters 1–20 from Figures 6A–C as assayed by gene expression microarrays. For MEFs, gene expression levels are based on Supplemental Table 2 of Sridharan et al (Sridharan et al., 2009). Heatmaps below the bar graphs show the relative replication timing of EBM9/NPC (N), Gsc+Sox17– Mesoderm (Me), Gsc+Sox17+ Endoderm (En) and MEF (F) compared to ICM cell types (=ESC/iPSC). Note that an earlier replication timing shift (red) is associated with high ratios of up- to down-regulation, while a later replication timing shift (green) is associated with higher percentages of down-regulation compared to up-regulation.

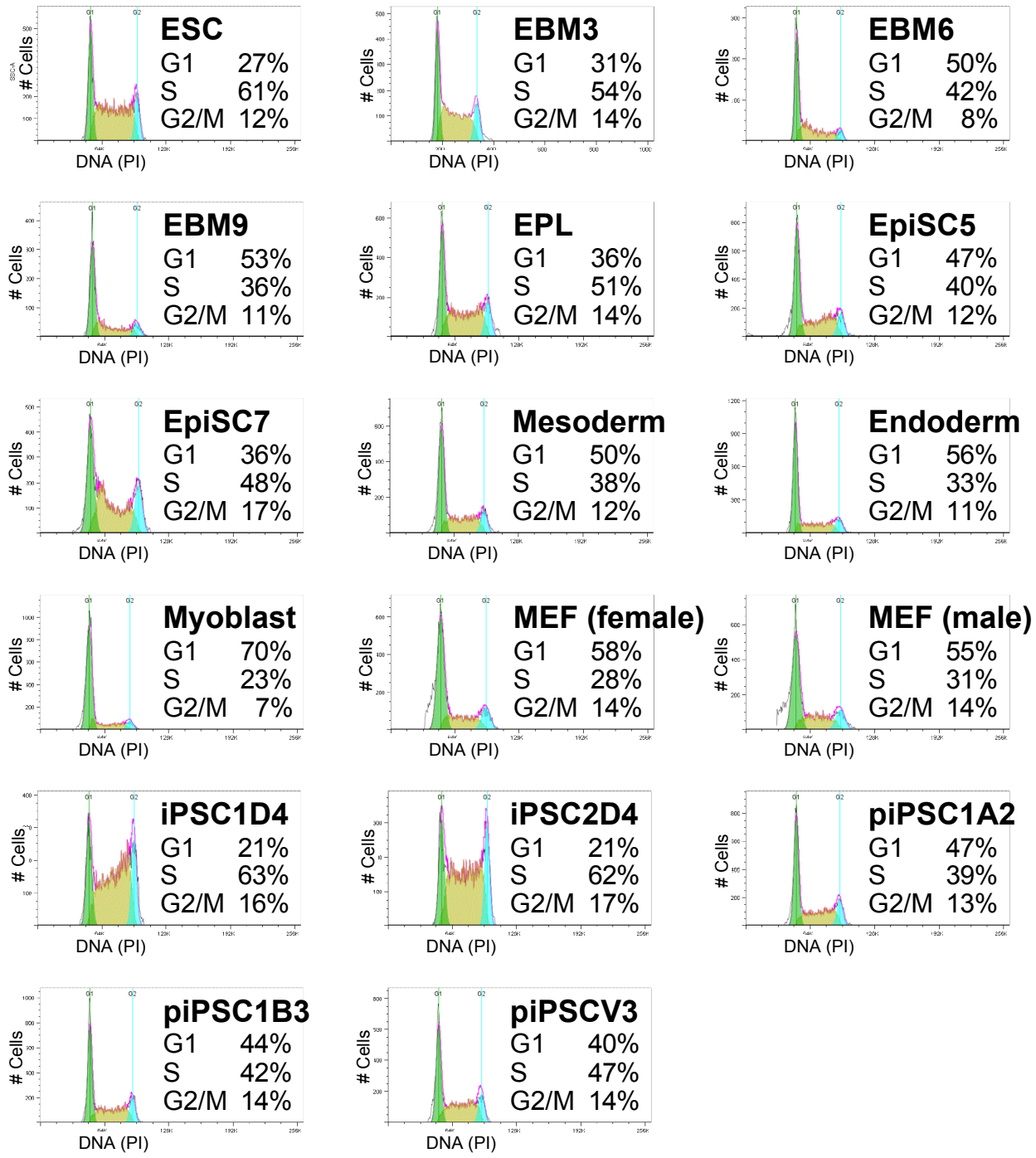

Supplemental Figure 14. Cell Cycle Profiles by Flow Cytometry
Cell cycle analysis was done with the FlowJo software using the Watson model. Note the increase in %G1-phase and decrease in %S-phase during the transition from ICM/early epiblast (ESC, iPSC, EBM3 and EPL) to late epiblast and beyond (EpiSC, EBM6, EBM9, Gsc+Sox17– Mesoderm, Gsc+Sox17+ Endoderm, Myoblast, MEF and piPSC).